Stretching of homopolymers and contact order

Marek Cieplak,[1] Trinh Xuan Hoang,[2] and Mark O. Robbins[3]

[1]*Institute of Physics, Polish Academy of Sciences, Al. Lotników 32/46, 02-668 Warsaw, Poland*
[2]*Institute of Physics and Electronics, Vietnamese Academy of Science and Technology, 10 Dao Tan, Ba Dinh, Hanoi, Vietnam*
[3]*Department of Physics and Astronomy, The Johns Hopkins University, Baltimore, Maryland 21218, USA*

Mechanical stretching of self-interacting homopolymers is studied through molecular dynamics simulations in which the polymers are pulled with constant speed. At temperatures below the compactification temperature, the force-extension curves show a plateau that corresponds to the situation in which the polymer adopts "ball-string" configurations. The dependence of rupture distances on contact order and the effects of temperature are similar to those found in the case of model proteins. The dependence of behavior on the pulling speed is logarithmic. In the entropic limit, above the compactification temperature, the rupturing of contacts shows a monotonic decrease of extension with the contact order. The attainment of this limit depends on the system size and the pulling speed.

PACS number(s): 87.15.La, 87.15.He, 87.15.Aa

I. INTRODUCTION

Recently, there have been many experimental studies of mechanical stretching of single biomolecules, such as strands of DNA [1–3], and of large multidomained proteins [4,5]. The force (F)–displacement (d) curves of proteins are specific, intricate, and reproducible so that they can be thought of as fingerprints of the proteins [6]. In addition, theoretical studies [7–9] show that the stretching scenarios are complex and not directly related to the folding scenarios. These scenarios can be characterized by diagrams which show an average displacement at which a contact interaction is ruptured (or, in the case of folding, an average time needed to establish a contact) as a function of the contact order, i.e., of the sequential distance between two amino acids that interact in the native state. Even though the F-d patterns and the stretching scenarios show dependence on the pulling speed and on the stiffness of the pulling device [7], they are governed primarily by the specific set of interactions that produce the unique folded structure of the protein.

In this paper, we discuss mechanical stretching of molecules without specific interactions: single self-associating homopolymers whose monomers all interact with each other. One goal is to determine how the behavior of molecules with nonspecific interactions contrasts with that of proteins. In addition, self-interacting homopolymers can be considered as models of DNA strands, which show much less specificity than any protein. They also model polymeric chains, and the mechanical properties of PNIPAM [poly(N-isopropyl acrylamide] and PEO [poly(ethylene oxide)] have been studied recently using atomic force microscopy [10].

Theoretical studies of homopolymer stretching have begun from simple models that are amenable to analytical treatments, such as the freely jointed chain (FJC) and the wormlike chain (WLC) [11]. The formula for the force in the WLC model, derived within the continuous chain approximation [12], has been widely used to fit experimental F-d curves for a variety of biomolecules including DNA [13], RNA [14], and proteins. Recently, a more general solution [15] of the

WLC model, which takes into account the discreteness of the chain, has been given. This generalized formula can be used to fit the experimental data on single and double stranded DNA in the intermediate and high force regimes, and at the same time gives extra information on the intrabead distance along the chain. Furthermore, it predicts the existence of a crossover force, above which the WLC force approaches the FJC result [15].

The WLC model ignores self-avoidance and attractive interactions between different segments of the chain. Thus it can be applied only in the case of stretching under good solvent conditions, i.e., above the θ transition [11] temperature T_θ. Under poor solvent conditions, theoretical studies of homopolymer stretching are usually confined to mean-field [16,17] or lattice [18–20] models. A common characteristic of such studies is that at temperatures below T_θ they predict existence of a plateau region associated with a well defined force in the F-d curve. The collapse-coil transition at this force is found to be first [16,20,18] and second order [18,19] in three and two dimensional models, respectively.

The studies described above usually refer only to cases in which the polymer is being pulled with a fixed force. However, in typical experimental pulling setups, like in the atomic force microscope, the conditions correspond to a cantilever that has a certain stifness and that moves with a certain speed. This is neither the fixed force nor the fixed extension situation. Furthermore, the analytically derived results adopt equilibrium conditions whereas the speed with which the cantilever moves may often significantly exceed the relaxation rate of the system, especially at low temperatures. Thus establishing the theoretical pulling rate dependence of the stretching process is of interest.

Here, we present results that are based on molecular dynamics simulations of self-attracting Lennard-Jones homopolymers which are stretched by a cantilever moving at a constant speed and at temperatures which can be lower than T_θ. The simulations are similar to our previous studies of stretching in a Go-like model of proteins [7–9,21]. We show that the stretching behavior of homopolymers is different from that of proteins in that there are no characteristic large

peaks in the *F-d* curves. Instead, variations in the pattern are more regular, of a smaller scale, and thus more akin to the features found when stretching model secondary structures of proteins [7,21]. This bland behavior arises primarily because, in homopolymers, interactions of all contact orders are present through most of the pulling process. However, the changes brought about by increasing temperature are analogous to those occurring in proteins: the *F-d* curves gradually lose whatever mild features they had as *T* rises.

An interesting feature of the force-displacement curves is a pronounced plateau. The plateau grows in extent with increasing chain length and is similar to that observed in an experimental study of PNIPAM [10]. Direct spatial analysis shows that the homopolymer is in a "ball-string" configuration. Such a configuration has already been observed by Maurice and Matthai [22] in molecular-dynamics studies of a homopolymer with the Morse-potential-based interactions under poor solvent conditions and by Kreitmeier *et al.* [23] in Monte Carlo studies of a Lennard-Jones system. The plateau force corresponds to that needed to pull a monomer out of a compact molten globule into an extended chain. It is thus related to the surface tension of the polymer droplet and decreases slowly as the droplet shrinks. It also decreases with increasing temperature, and disappears above a characteristic unfolding temperature.

We also study the unraveling scenarios by monitoring the distances at which each contact breaks for the last time. We show that the scenario diagrams shift logarithmically with pulling rate and they become increasingly simplified as the temperature is raised. In the entropic limit [9] the rupture distances become strictly monotonic as a function of the contact order so that the longest ranged contacts break first. This limiting high temperature behavior is very similar to that found for proteins [9].

The following section describes the model interactions and geometry used in our simulations. Section III presents results for thermal unfolding, force-extension curves, and stretching scenarios. We conclude that despite the lack of specificity, the qualitative stretching behavior of self-interacting homopolymers is similar to that of proteins.

II. MODEL

We consider a linear chain of *N* beads of mass *m*. The beads are tethered together by stiff harmonic potentials with minima located at a proteinlike distance of 3.8 Å. Nonspecific Lennard-Jones 6-12 potentials provide attraction between all nonconsecutive beads. The energy and length parameters of the Lennard-Jones potential are denoted by ϵ and σ, respectively. Note that there are two distance scales in this model, the tethering length and the attraction range. We choose $\sigma=5$ Å so that both distances are typical of proteins, and present our results with lengths in units of Å. The main difference from Go-like models of proteins is that we include attractive interactions between all beads, rather than only at native contacts.

The simulation method is similar to our previous molecular-dynamics (MD) studies of proteins [7–9,24–27]. In particular, the equations of motion are integrated using a
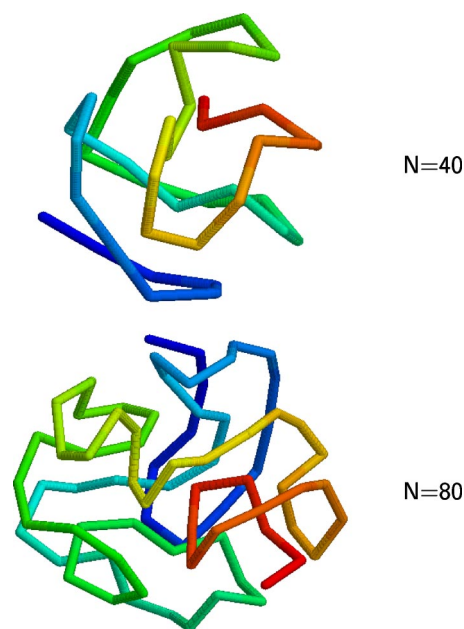
FIG. 1. Examples of folded homopolymer conformations as obtained by annealing. The system sizes are indicated.

fifth order predictor-corrector algorithm [28]. The time step is 0.005 τ, where $\tau \equiv \sqrt{m\sigma^2/\epsilon}$ is the characteristic time for the Lennard-Jones potential. The effective temperature is given by the ratio $\widetilde{T} \equiv k_B T/\epsilon$, where *T* is the temperature and k_B is Boltzmann's constant. Constant temperature is maintained with a Langevin thermostat [29]. The damping rate, $\gamma=2m/\tau$, is chosen to be large enough to produce the overdamped dynamics typical of chain molecules in a solution, without slowing the dynamics unnecessarily.

The initial compact state of the homopolymer is obtained by annealing the system at progressively lower temperatures. While this state is only one of many local energy minima, it is used for all runs at a given *N* in order to minimize fluctuations due to initial conditions. Examples of such states are shown in Fig. 1. The terminal beads are more likely to lie at the surface of the initial state for entropic reasons, and were always at the surface in the clusters considered here.

The polymer is stretched by attaching both ends of the polymer to harmonic springs of spring constant *k*. The other end of one spring is held fixed. The outer end of the other is pulled at constant speed v_p in the direction of the initial end-to-end vector of the polymer. The displacement of the pulled end of the spring is denoted by *d*. The net force acting on the bead attached to the moving end is denoted by *F* and is measured from the extension of the pulling spring. The force on the other end bead is nearly the same, indicating that the system is quasistatic from the point of view of stress transfer. *F* is averaged over a time interval of 100τ which, for a typical pulling speed of 0.005 Å/τ, corresponds to a displacement of 0.5 Å. The averaging is performed in order to reduce thermal noise without substantially affecting the spatial resolution. We consider two values of stiffness of the pulling springs. The stiff spring case corresponds to *k* $=100\epsilon/$Å^2. The contrasting soft spring case corresponds to $k=0.1\epsilon/$Å^2.

The unfolding scenario is specified by the unbinding or breaking distance d_u for all contacts. A contact between beads i and j is considered ruptured if the distance between them exceeds 1.5σ. Note that at a finite temperature the contact may break and reform several times and d_u is taken to be associated with the final rupture.

III. RESULTS

A. Thermal unfolding

In the limit of infinite chain length there is a sharp transition in the scaling behavior of associating polymers at the theta temperature T_θ. Below this temperature the polymer has a compact, globular structure at large scales with the radius of gyration R_g scaling as $N^{1/3}$. Above T_θ the polymer has the statistics of a self-avoiding random walk with $R_g \sim N^{0.588}$. At T_θ, the polymer follows simple random walk statistics: $R_g \sim N^{1/2}$. The transition at T_θ is often referred to as the globule-coil transition.

Graessley *et al.* [30] have considered a model similar to ours, but with the Lennard-Jones interaction truncated at $2.5\ \sigma$. From the scaling behavior for $N \geqslant 200$ they determined $\widetilde{T}_\theta = 3.18$. We expect that the untruncated interactions considered here should lead to an increase in $\widetilde{T}_\theta$. However, we focus on the much shorter chain lengths typical of proteins, where finite size may also produce significant shifts in the characteristic temperature.

Figure 2 shows the radius of gyration as a function of temperature for three different chain lengths. We identify a characteristic unfolding temperature $\widetilde{T}_u$ for each N with the point of inflection of the corresponding curve. The value of $\widetilde{T}_u$ increases from about 2.8 to 3.4 to 4.0 as N increases from 40 to 80 to 120. This suggests, as expected, that $\widetilde{T}_\theta$ is higher than that obtained for truncated interactions [30].

For the chain lengths considered here, we find that $\widetilde{T}_u$ correlates with changes in the thermal and mechanical response. Figure 2 also shows the specific heat of the polymer as a function of $\widetilde{T}$. Note that there is a small bump at the N dependent value of T_u. The transition at this temperature can be viewed as analogous to a liquid-vapor transition where the polymer expands from one disordered state to another of lower density. The maximum in the specific heat occurs at a much lower temperature $\widetilde{T}_{\max} \approx 0.26$. Examination of the polymer dynamics shows that this corresponds to something like the glass transition temperature. The polymer is trapped in local energy minima for long periods of time for $T < \widetilde{T}_{\max}$ and moves freely between configurations at higher temperatures.

Previous work for a homopolymer with attractive square-well potentials [31] also found $\widetilde{T}_{\max} \ll \widetilde{T}_u$. It is interesting to note that proteins show very different behavior. Due to a high synchronology between the collapse and folding transitions $\widetilde{T}_\theta$ is generally close to $\widetilde{T}_{\max}$. In some theoretical works it has actually been assumed that $\widetilde{T}_{\max}$ exactly coincides with the θ transition in proteins [32].
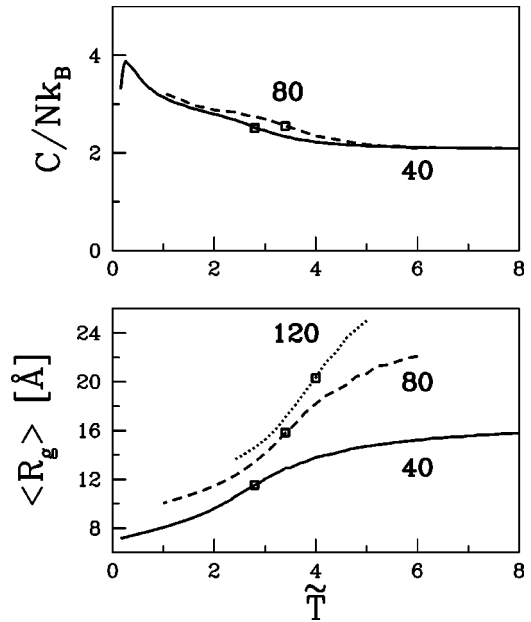
FIG. 2. The temperature dependence of the heat capacity C and the averaged radius of gyration $\langle R_g \rangle$ for the homopolymers of sizes that are indicated. (C for $N=120$ is not shown to avoid overcrowding of the figure.) The error bars are of the order of the thickness of the lines. The square symbols show the unfolding temperature T_u. The data shown are obtained by averaging over n_t annealing trajectories where $n_t = 50$, 50, and 25 for $N=40$, 80, and 120, respectively. Each trajectory starts from a random open conformation and the reduced temperature $\widetilde{T}$ is decreased in steps of 0.1. After an equilibration time of $1000\ \tau$ the energy and the radius of gyration are averaged over a time between 2000 and $10\,000\tau$ depending on the temperature.

B. Force-displacement curves

Figure 3 shows examples of single trajectory F-d curves corresponding to unraveling of the $N=40$ homopolymer. We consider temperatures below and above $\widetilde{T}_{\max}$ and two values of the cantilever spring, the stiff and the soft cases defined in Sec. II.

At low temperatures F-d curves show regions of constant upward slope where the polymer is trapped in a local free energy minimum, followed by rapid drops where individual bonds break. The sawtooth structure is more pronounced for the soft cantilever. The slope of the upward ramps is just the combined effective stiffness of the springs and polymer. The softer the cantilever, the longer the distance needed to reach the force where bonds break. The extension required for the force to decrease is also larger. As a result, bonds that break sequentially with a stiff spring all break in the same event when a soft spring is used.

The pattern of F-d curves is a fingerprint for the initial conformation, since the sequence of broken bonds depends on the initial structure and the direction of pulling. Unlike proteins, the initial conformation of homopolymers is not unique, and different random initial configurations lead to very different patterns. In proteins, one also typically observes larger and more well-defined peaks [4,5,8,9,33–35]. The cooperative nature of the bonds results in an unusually
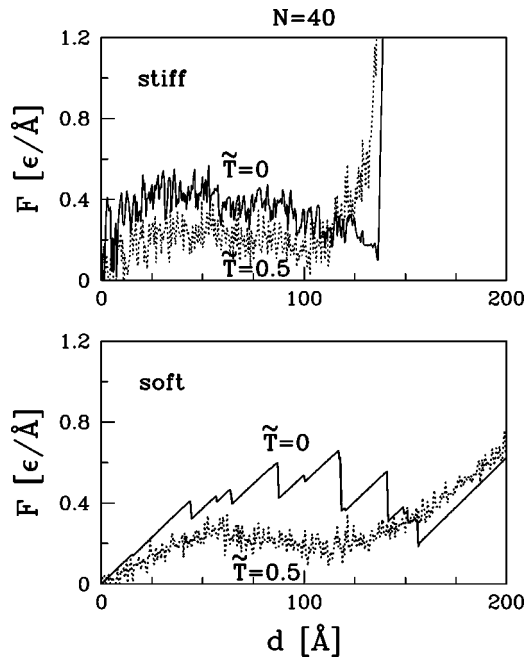
FIG. 3. The F-d curves for an $N=40$ homopolymer system. The values of $\widetilde{T}$ are indicated. The pulling speed is 0.005 Å$/\tau$. The upper panel shows pulling with a stiff cantilever ($k_c=100\epsilon/\text{Å}^2$) whereas the lower panel corresponds to the soft cantilever ($k_c=0.1\epsilon/\text{Å}^2$).

deep metastable free energy minimum for the native state. This in turn leads to more simultaneous bond breaking and larger forces. For example, when the same Lennard-Jones potential is used to couple native contacts in a model of a domain of titin ($N=89$) [8,21], the peak force is an order of magnitude larger ($4\epsilon/\text{Å}$) than for homopolymers. Of all the model proteins considered [7,9,21], only simple secondary structures, which are known to have less inhomogeneity in binding forces, produce peak forces that are almost as small as those in Fig. 3.

When the temperature increases beyond $\widetilde{T}_{\max}$ the homopolymer can sample many conformations during unfolding. Thus the curves at $\widetilde{T}=0.5$ show no clear peaks, just thermal fluctuations that do not correlate with the initial state. Force-displacement curves for proteins also show a general loss of structure with increasing $\widetilde{T}$ [9,21]. However, the specific interactions of proteins lead to much higher values of $\widetilde{T}_{\max}$ (~ 1) even for the same interaction energies [21]. This reflects the unusually deep binding energy of the native state.

For all temperatures the force curves in Fig. 3 show a general tendency to increase and then drop before a final rapid rise. On increasing d from 0, there is a gradual buildup in the force. The weakest bonds tend to break first, although their location relative to the pulling force is also important [21]. The forces later decrease because there are fewer remaining bonds to hold the globular portion of the polymer together. Eventually, all the Lennard-Jones bonds are ruptured, and the polymer is fully extended. The pulling force then acts exclusively to stretch the harmonic tethering forces, producing the final rapid rise in force.
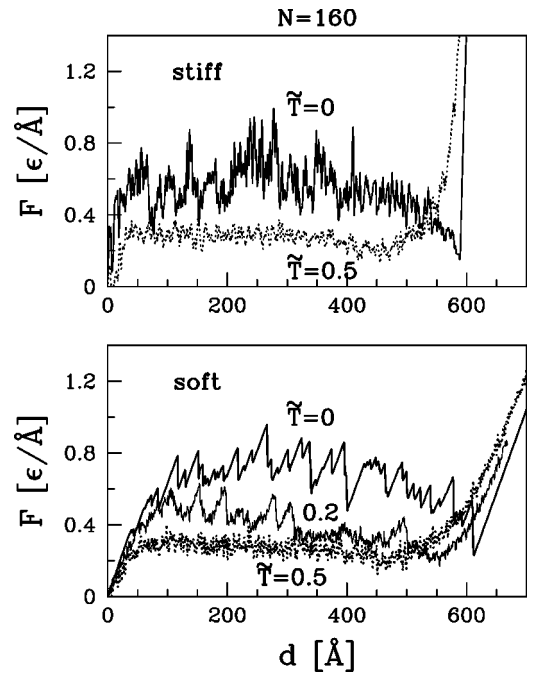
FIG. 4. Similar to Fig. 3 but for an $N=160$ homopolymer system.

Figure 4 shows how the force curves evolve as N is increased from 40 to 160. The increased length leads to many more metastable states. As a result the force curves at $\widetilde{T}=0$ show a roughly four-fold increase in the number of peaks for each value of the spring constant. Peaks are still evident at $\widetilde{T}=0.2$, which is slightly below $\widetilde{T}_{\max}=0.26$. However, thermal fluctuations reduce the force needed to rupture bonds and remove some of the metastable states. Curves for $\widetilde{T}=0.5 \gg \widetilde{T}_{\max}$ show only thermal fluctuations superimposed on a broad plateau followed by a final rapid rise. As for $N=40$, there is a gradual drop in the force along the plateau that is related to a gradual decrease in the number of bonds. Figure 5 shows that both the length of the plateau and the plateau force gradually decrease with increasing temperature. By $\widetilde{T}=4 \approx \widetilde{T}_u$ there is little evidence of a plateau and the entire curve can be fit to a monotonically increasing WLC force.

The origins of the plateau and its temperature dependence can be determined by examining the conformation of the polymer. Examples of conformational changes during stretching at four values of $\widetilde{T}$ are shown in Fig. 6. In each case the polymer contains linear regions on either side of a compact globule. (We have not seen configurations with multiple globules, which would have higher surface energy.) As the polymer is extended, monomers are pulled out of the globule and into the linear regions. The required force drops as the globule shrinks because the increase in curvature leads, on average, to fewer bonds to other monomers.

For $\widetilde{T} > \widetilde{T}_{\max}$ there are rapid rearrangements of bonds within the globule, indicating that it is in a molten state. Some mobility is also observed at $\widetilde{T}=0.2$, but the degree of mobility decreases with further decreases in $\widetilde{T}$. The linear regions in Fig. 6 become more crooked with increasing tem-
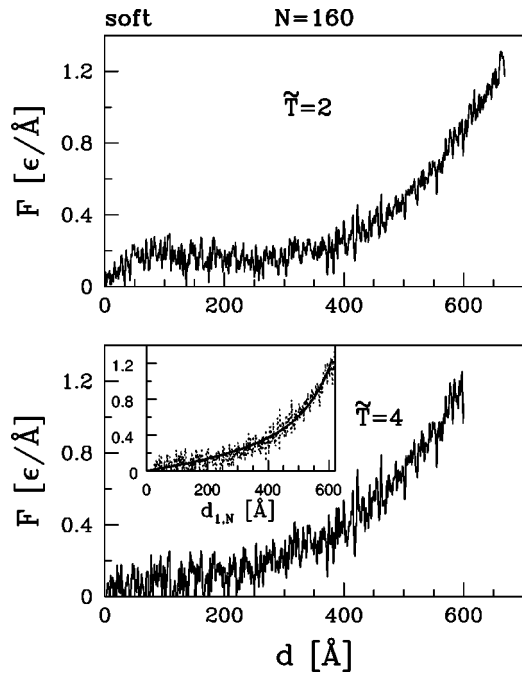
FIG. 5. Examples of the F-d curves obtained at $\tilde{T}$ of 2 and 4 for the $N=160$ system pulled by a soft spring. Inset: the force vs the end-to-end distance $d_{1,N}$ at $\tilde{T}=4$ is fitted by the WLC equation, $F=(\tilde{T}/4p)[(1-d_{1,N}/L)^{-2}-1+4d_{1,N}/L]$, using the contour length $L=840$ Å and the persistence length $p=12.3$ Å. The finite persistence length is due to local steric repulsion in the chain. The end-to-end distance was computed as $d_{1,N}=d+d_0-F/k$, where d_0 is the initial end-to-end distance and k is the cantilever spring constant.

perature as their entropy becomes more important. This also increases the amount of polymer in the linear region at a given extension, leading to a decrease in globule size with increasing $\tilde{T}$ in Fig. 6. The interface of the globule also becomes more diffuse with increasing $\tilde{T}$. This reflects a drop in surface tension that corresponds to the drop in plateau force needed to extend the linear region.
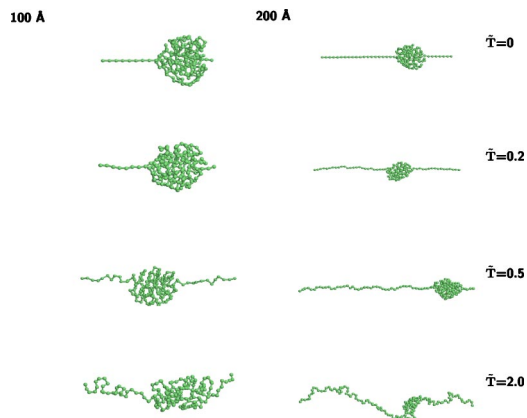
FIG. 6. Snapshots of a $N=160$ system stretched by distances of 100 and 200 Å are shown in the left and right hand panels, respectively. The pulling springs are soft and the pulling speed $v_p=0.005$ Å$/\tau$. The value of $\tilde{T}$ is 0, 0.2, 0.5, and 2.0 as one goes from top to bottom.

Plateau forces have also been observed in recent atomic force microscopy (AFM) studies of PNIPAM and PEO polymers under poor solvent conditions [10]. These authors proposed that the mechanism for the observed plateau is analogous to the Rayleigh instability, which can lead to a "ball-spring" configuration like those shown in Fig. 6. In their experimental setup, however, the ball-spring configuration is not attained. Instead a stretched configuration is found between two globules which are bound to the AFM tip and a flat surface. Although the analogy is presumably correct, they did not consider the possible change in force with decreasing droplet size that we find in our simulations.

The existence of a plateau in the F-d curve has been predicted in several theoretical studies [16,18–20] when the polymer is stretched under the strictly fixed force conditions. Our results show that the plateau can be also observed under constant speed conditions. Pulling with a cantilever can be considered as intermediate between the fixed force and fixed stretch cases, approaching a fixed force for a soft cantilever and a fixed stretch for a stiff cantilever. Note that the plateau is not observed in the case of proteins when they are pulled with a constant speed [8,21]. Thus even though there is a general difference between the fixed force and fixed stretch ensembles [36], this difference seems to be much smaller in the case of homopolymers than in the case of proteins.

C. Stretching scenarios

We now consider the succession of unraveling events in a homopolymer. The contact order of a bond between the ith and jth monomer along the homopolymer is given by the sequential separation $|j-i|$. The unfolding scenario is represented as a plot of the displacement of the pulling spring d_u at which the bond ruptures for the last time against contact order. In proteins at $\tilde{T}=0$ such plots form complex patterns in the $d_u,|j-i|$ plane [8,9]. In most cases the long range contacts tend to break first and the short range contacts break throughout the process. There are generally pronounced striations where clusters of bonds in different secondary structures unravel. This type of structure is absent in the results for homopolymers shown in the top left panel of Fig. 7. Instead the points fill a whole triangular region. This means that there is no correlation between the contact order and d_u. Note that the number of bonds in proteins is much smaller, leading to sparser scenario diagrams.

As $\tilde{T}$ increases, the scenarios occupy progressively smaller regions of the $d_u,|j-i|$ plane. In the high temperature limit, the plots collapse onto a line with d_u decreasing monotonically with increasing $|j-i|$. In this limit the initial conformation of the polymer is irrelevant and the stretching scenario is governed entirely by the contact order. Studies at different temperatures indicate that for homopolymers this entropic behavior sets in near the unfolding temperature T_u (Fig. 1), at least at sufficiently slow pulling rates.

The results in Fig. 7 are for $v_p=0.005$ Å$/\tau$. Figure 8 shows $d_u,|j-i|$ patterns for $N=40$ homopolymers at $\tilde{T}=2$ with v_p: 0.0005, 0.005, and 0.05 Å$/\tau$. Figure 9 shows data corresponding to two lower velocities values: 0.001 and 0.01 Å$/\tau$ but averaged over contacts of two fixed sequence
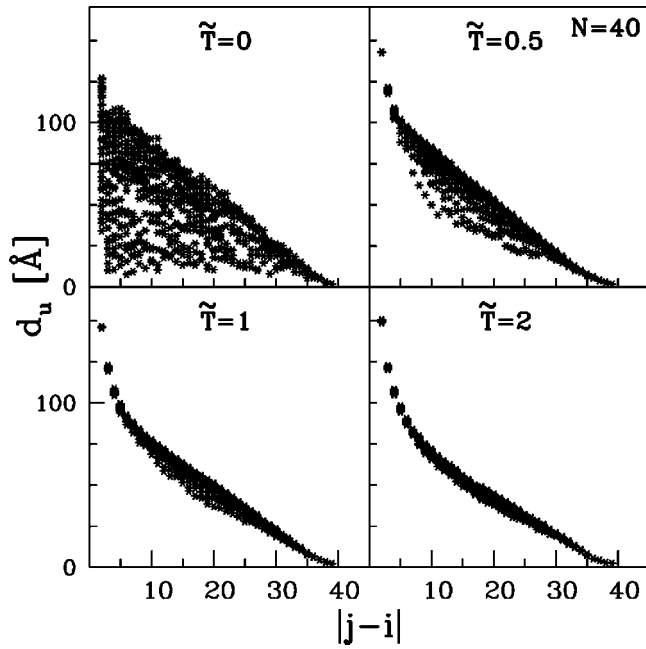
FIG. 7. Scenarios of mechanical unfolding averaged over 20 homopolymers with $N=40$ for the temperatures indicated. For each homopolymer, one stretching trajectory is considered. The pulling speed is 0.005 Å$/\tau$.

distances of 10 and 20. Figures 8 and 9 combined together indicate a logarithmic dependence of the pattern on v_p in the entropic limit. It is interesting to note that the amplitude of the logarithmic dependence is a nonmonotonic function of
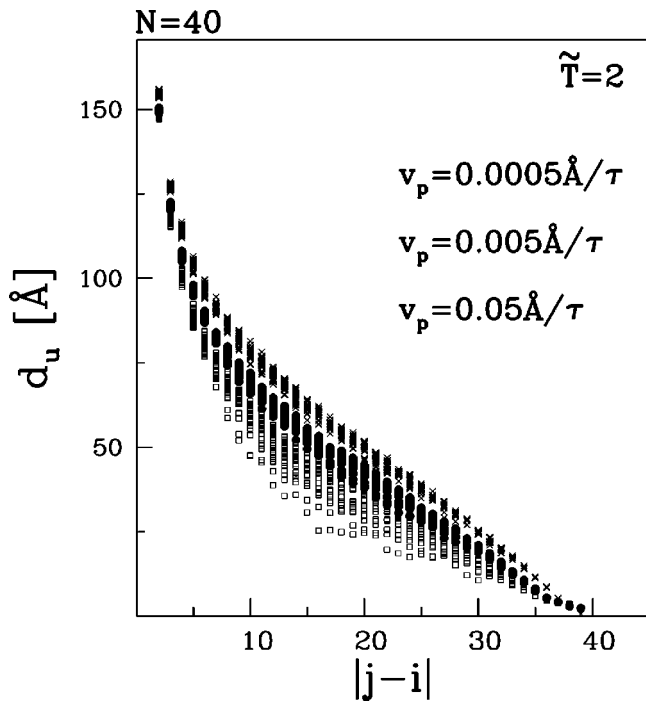
FIG. 8. Scenarios of mechanical unfolding of the $N=40$ homopolymers at three indicated values of the pulling speed. The crosses, black circles, and open squares correspond to v_p of 0.0005, 0.005, and 0.05 Å$/\tau$, respectively.
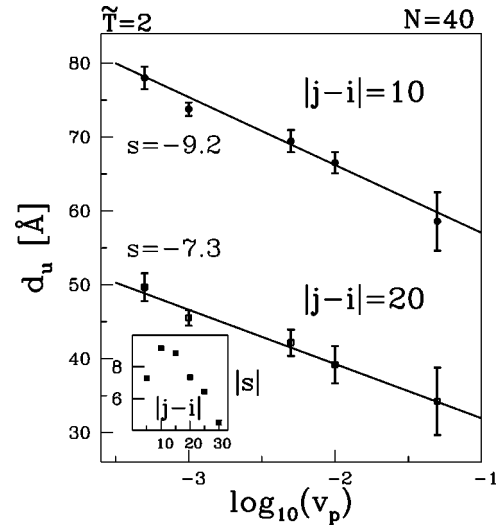
FIG. 9. The logarithmic dependence of d_u on v_p for $N=40$. The results corresponding to a given value of $|j-i|$ are averaged along the chain, i.e., averaged along the vertical lines in Fig. 8. The lines have slopes s that are indicated. The inset shows the absolute values of the slope for selected values of $|j-i|$.

$|j-i|$, as indicated in the inset of Fig. 9. For N of 40, there is a maximal sensitivity to v_p around $|j-i|$ of 10 and essentially no sensitivity around the terminal values of $|j-i|$. Figure 10 implies that the location of the maximum moves up on increasing the system size.

The logarithmic dependence on v_p can be explained in the following way. We note that the upper bound of the triangular regions shown in Figs. 7 and 8 is a straight line, $d_u=N-|j-i|$, that corresponds to a situation in which the polymer is perfectly straight on either side of a given contact. For a randomly fluctuating polymer, however, this is an extremely unlikely situation. At sufficiently high temperatures, the sampling of conformations takes place with equal probablity and the lower the pulling speed, the longer time to sample conformations. One can expect that getting to states near the
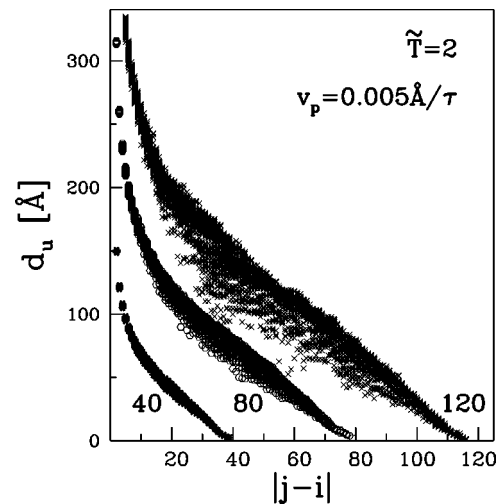
FIG. 10. Scenarios of mechanical unfolding for the three indicated system sizes and at a fixed value of $\tilde{T}$ of 2.
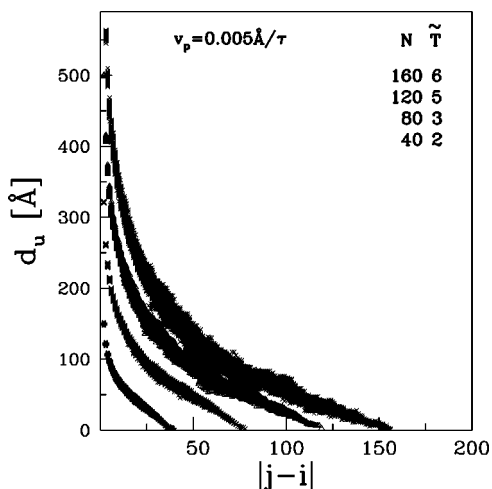
FIG. 11. Scenarios of mechanical unfolding for the four indicated system sizes and adjusted indicated values of $\widetilde{T}$. The legend corresponds to the data points in a top-to-bottom way.

upper bound is exponentially unlikely. In other words the time to achieve the upper bound will be exponentially long. Let X denote the distance moved toward the upper bound. Then the probability of finding a state with that distance would be $P \propto \exp(-X/C)$, where C is a constant that varies along the upper bound. The probability of sampling of conformations is proportional to $1/v_p$. This means that $P \propto \exp(-X/C) \propto v_p^{-1}$. Thus $X \propto \ln(v_p)$, where the coefficient of proportionality depends on $|j-i|$.

We now demonstrate that the attainment of the entropic limit for a given v_p depends on the system size. This is illustrated in Figs. 10–12 which correspond to $v_p = 0.005\text{Å}/\tau$. Figure 10 considers $\widetilde{T}=2$ for which the $N=40$ stretching scenario is almost perfectly monotonic. Increasing N at the fixed value of $\widetilde{T}$ results in a gradual blurring of the monotonic pattern. This blurring, or broadening, of the pattern can be countered by considering still higher values of $\widetilde{T}$ as shown in Fig. 11. It is expected that a similar effect can be achieved by reducing the pulling speeds.

It should be noted that the entropic limit corresponds to sampling of all conformations of the chain. Thus the longer the chain, the longer time is needed to probe the conformations. In order to observe the entropic behavior during stretching, v_p must be small enough to allow for sampling of the ensemble over a small fraction of the stretching time. Thus longer chains reach the entropic limit at lower v_p for a given $\widetilde{T}$ or higher $\widetilde{T}$ for a given v_p.

A scaled version [9] of the data shown in Fig. 11 is shown in Fig. 12. It is seen that the order of the scenario lines is
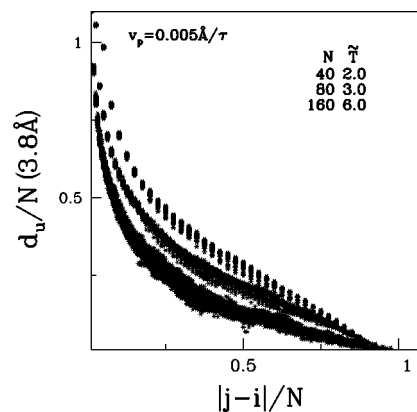
FIG. 12. A scaled representation of the stretching scenarios of the three sets of data shown in Fig. 12. The legend corresponds to the data points in a top-to-bottom way.

inverted compared to the order found in Fig. 11. For each N, $\widetilde{T}$ is large enough to limit the scatter of points around a monotonically decreasing curve. However, the curves move farther from the limiting straight line $d_u = N - |j-i|$ as N increases, because such rare fluctuations are more unlikely for longer chains.

In conclusion, we have computed $E-d$ curves and unfolding scenarios for homopolymers over a wide range of rates, chain lengths, and effective temperatures. Trends with these parameters are similar to those found for model proteins [7–9], but the greater specificity of protein structures leads to larger unbinding forces and temperatures. The substantially greater statistics of bonds in homopolymers facilitates studies of the logarithmic rate dependence of unfolding and the sensitivity to chain length. Homopolymers exhibit a clear force plateau that is related to partial unfolding into a ball-string structure. It is normally assumed that once proteins start to unfold they lose all internal structure. The persistence of a ball-string structure in homopolymers suggests that protein unfolding need not have an all or nothing character.

[1] U. Bockelmann, B. Essevaz-Roulet, and F. Heslot, Phys. Rev. Lett. **79**, 4489 (1997).

[2] C. G. Baumann, V. A. Bloomfield, S. B. Smith, C. Bustamante, M. D. Wang, and S. M. Block, Biophys. J. **78**, 1965 (2000).

[3] U. Bockelmann, Ph. Thomen, B. Essevaz-Roulet, V. Viasnoff, and F. Heslot, Biophys. J. **82**, 1537 (2002).

[4] M. Rief, M. Gautel, F. Oesterhelt, J. M. Fernandez, and H. E. Gaub, Science **276**, 1109 (1997); A. F. Oberhauser, P. E.

Marszalek, H. P. Erickson, and J. M. Fernandez, Nature (London) **393**, 181 (1998); M. Rief, J. Pascual, M. Saraste, and H. E. Gaub, J. Mol. Biol. **286**, 553 (1999).

[5] G. Yang, C. Cecconi, W. A. Baase, I. R. Vetter, W. A. Breyer, J. A. Haack, B. W. Matthews, F. W. Dahlquist, and C. Bustamante, Proc. Natl. Acad. Sci. U.S.A. **97**, 139 (2000).

[6] H. Li, M. Carrion-Vazquez, A. F. Oberhauser, P. E. Marszalek, and J. M. Fernandez, Nat. Struct. Biol. **7**, 1117 (2000).

[7] M. Cieplak, T. X. Hoang, and M. O. Robbins, Proteins: Struct., Funct., Genet. **49**, 104 (2002); **49**, 114 (2002).

[8] M. Cieplak, T. X. Hoang, and M. O. Robbins, Proteins: Struct., Funct., Genet. **49**, 114 (2002).

[9] M. Cieplak, T. X. Hoang, and M. O. Robbins, Phys. Rev. E **69**, 011912 (2004).

[10] B. J. Haupt, T. J. Senden, and A. M. Sevick, Langmuir **18**, 2174 (2002).

[11] M. Doi and S. F. Edwards, *Theory of Polymer Dynamics* (Oxford University Press, Oxford, 1988).

[12] J. F. Marko and E. D. Siggia, Macromolecules **28**, 8759 (1995).

[13] C. Bouchiat and M. Mezard, Phys. Rev. Lett. **80**, 1556 (1998).

[14] U. Gerland, R. Bunschuh, and T. Hwa, Biophys. J. **84**, 2831 (2003).

[15] A. Rosa, T. X. Hoang, D. Marenduzzo, and A. Maritan, Macromolecules **36**, 10 095 (2003).

[16] A. Halperin and E. B. Zhulina, Europhys. Lett. **15**, 417 (1991).

[17] P. L. Geissler and E. Shakhnovich, Phys. Rev. E **65**, 056110 (2002).

[18] P. Grassberger and H.-P. Hsu, Phys. Rev. E **65**, 031807 (2002).

[19] D. Marenduzzo, A. Maritan, and F. Seno, J. Phys. A **35**, L233 (2002).

[20] D. Marenduzzo, A. Maritan, A. Rosa, and F. Seno, Phys. Rev. Lett. **90**, 088301 (2003).

[21] M. Cieplak, T. X. Hoang, and M. O. Robbins, Proteins: Struct., Funct., Bioinf. **56**, 285 (2004).

[22] R. G. Maurice and C. C. Matthai, Phys. Rev. E **60**, 3165 (1999).

[23] S. Kreitmeier, M. Wittkop, and D. Goerlitz, Phys. Rev. E **59**, 1982 (1999).

[24] T. X. Hoang and M. Cieplak, J. Chem. Phys. **112**, 6851 (2000); **113**, 8319 (2001).

[25] T. X. Hoang and M. Cieplak, J. Chem. Phys. **113**, 8319 (2001).

[26] M. Cieplak and T. X. Hoang, Proteins: Struct., Funct., Genet. **44**, 20 (2002).

[27] M. Cieplak and T. X. Hoang, Biophys. J. **84**, 475 (2003).

[28] M. P. Allen and D. J. Tildesley, *Computer Simulation of Liquids* (Oxford University Press, New York, 1987).

[29] G. S. Grest and K. Kremer, Phys. Rev. A **33**, 3628 (1986).

[30] W. W. Graessley, R. C. Hayward, and G. S. Grest, Macromolecules **32**, 3510 (1999).

[31] Y. Zhou, C. K. Hall, and M. Karplus, Phys. Rev. Lett. **77**, 2822 (1996).

[32] D. K. Klimov and D. Thirumalai, Phys. Rev. Lett. **76**, 4070 (1996).

[33] P. E. Marszalek, H. Lu, H. B. Li, M. Carrion-Vazquez, A. F. Oberhauser, K. Schulten, and J. M. Fernandez, Nature (London) **402**, 100 (1999).

[34] H. Lu, B. Isralewitz, A. Krammer, V. Vogel, and K. Schulten, Biophys. J. **75**, 662 (1998).

[35] P. M. Williams, S. B. Fowler, R. B. Best, J. L. Toca-Herrera, K. A. Scott, A. Steward, and J. Clarke, Nature (London) **422**, 446 (2003).

[36] D. Keller, D. Swigon, and C. Bustamante, Biophys. J. **84**, 733 (2003).